Structure Control of Asymmetric Poly(vinyl butyral)-TiO_2 Composite Membrane Prepared by Nonsolvent Induced Phase Separation

Xunyao Fu,[1] Hideto Matsuyama,[1] Hideki Nagai[2]

[1]*Department of Chemical Science and Engineering, Kobe University, Kobe 657-8501, Japan*
[2]*Meisui Co., 1-27-6 Edohori, Nishi-ku, Osaka 550-0002, Japan*

Received 28 April 2007; accepted 5 September 2007
DOI 10.1002/app.27711
Published online 11 January 2008 in Wiley InterScience (www.interscience.wiley.com).

ABSTRACT: Poly(vinyl butyral) (PVB)-TiO_2 composite hollow fiber membranes were prepared via nonsolvent induced phase separation (NIPS). The membrane had a skin layer on both the outer and inner surface at the initial stage after membrane preparation. However, the outer surface became porous with the passage of time, as the polymer in the membrane's outer surface was decomposed by the photocatalysis of TiO_2. The initial water permeability increased with the increase of TiO_2 content. Furthermore, for all the membranes, as time elapsed the water permeabilities increased and became constant after about 15 days, which was in accordance with the alteration on the membrane's outer surface. Despite decomposition of the polymer on the outer surface, particle rejection hardly changed because the inner surface kept the original structure. Thus, addition of TiO_2 to the membrane is a useful way to improve water permeability while maintaining particle rejection. The clear asymmetric structure with both porous structure at the outer surface and skin layer at the inner surface was achieved by the addition of TiO_2. Therefore, the addition of TiO_2 is a new method for achieving the high porosity at the outer surface of the hollow fiber membrane. In addition, tensile strength and elasticity kept constant over time and were higher than those of original PVB membranes. © 2008 Wiley Periodicals, Inc. J Appl Polym Sci 108: 713–723, 2008

Key words: poly(vinyl butyral); nonsolvent induced phase separation; composite membrane; titanium dioxide; asymmetric structure

INTRODUCTION

The nonsolvent induced phase separation (NIPS) method is a popular way to prepare polymeric microporous membranes.[1–8] In the NIPS process, a homogeneous polymer solution is cast as a thin film or a hollow fiber shape, and then immersed into a nonsolvent coagulation bath. The diffusional exchange of solvent and nonsolvent across the interface between casting solution and nonsolvent can make the casting solution phase separate to form a membrane with a symmetric or asymmetric structure.

Poly(vinyl butyral) (PVB) is a product of the reaction between poly(vinyl alcohol) (PVA) and the butyl aldehyde in the presence of an acid catalyst. PVB can endure low temperature, light, change in humidity, bacteria and other microorganisms, alkali, and diluent acid.[9] Furthermore, PVB is hydrophilic to some degree since it retains a PVA part, which can reduce protein fouling caused by formation of cake on the hydrophobic membrane surface, and pore plugging or pore narrowing induced by particle aggregation inside the pores.[10–14] It has been reported that PVB had been used to prepare affinity membranes.[15] Shen et al.[8] and Jiang and coworkers[16] prepared PVB ultrafiltration membranes via NIPS. However, PVB is still a new material in the membrane preparation field and there are only a few papers on PVB membrane preparation. Previously, we prepared PVB hollow fiber membranes via thermally induced phase separation method.[17,18] Considering PVB is an attractive polymer material for membrane preparation, it is necessary to have further study on PVB membranes.

An asymmetric membrane combines the high selectivity of a dense membrane with the high permeation rate of a very thin membrane.[19,20] In industrial separation applications, an asymmetric membrane structure is desirable to minimize the resistance to transmembrane flow and the blocking of internal pores by solutes. To control asymmetric hollow fiber membrane structure, solvent is added into a coagulant bath[17,21] or water vapor is induced during air gap distance.[22] Moreover, some amount of additive such as low molecular weight component or a secondary polymer is frequently used for asymmetric membrane preparation.[23–26]

Correspondence to: H. Matsuyama (matuyama@kobe-u.ac.jp).

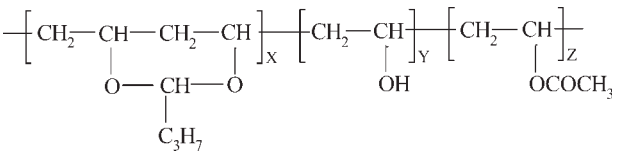

Figure 1 Structure of PVB.

In this study, TiO_2 nanoparticles were selected as such an additive. Titanium dioxide (TiO_2) has been the focus in numerous investigations recently because of its good photocatalytic and high hydrophilic properties, stable chemical property, innocuity, low cost, etc.[27,28] It has been reported that the addition of inorganic materials can improve the mechanical property of membranes,[25,29] and that the pore size and porosity on the membrane surface was increased.[30] In this work, TiO_2 nanoparticles were added into polymer solution to make an asymmetric membrane via the NIPS method. Clear asymmetric structure with both porous structure at the outer surface and skin layer at the inner surface was obtained because of the photocatalytic property of TiO_2. To compare the asymmetric structures obtained by various conditions, PVB concentration, the ratio of PVB to TiO_2, and the coagulation bath composition were changed.

EXPERIMENTAL

Materials

PVB (the degree of polymerization = 2400) was purchased from Denka (Japan). Vinyl butyral and vinyl alcohol parts of the copolymer are 81 and 17 wt %, respectively, and the residual vinyl acetate part is 2 wt %. The structure of PVB is shown in Figure 1. *N,N*-Dimethylacetamide (DMAc) was purchased from Wako Pure Chemical Industries (Japan). Anatase-type TiO_2 with a diameter of 180 nm was purchased from Tayca (Japan). All of the chemicals were used without further purification.

Hollow fiber membrane preparation

Hollow fiber membranes were prepared using a batch-type extruder. A measured amount of TiO_2 was dispersed into DMAc diluent. Ultrasonic vibration was applied to homogenize TiO_2 distribution in the diluent. After 1 h of ultrasonic vibration, the TiO_2-DMAc solution was stirred for 12 h at room temperature. Then PVB was mixed with the homogeneous TiO_2-DMAc solution and stirred at room temperature for 12 h. Homogenous PVB-TiO_2/DMAc solution was fed to the vessel, holding at room temperature for 30 min for defoaming. Then the homogeneous solution was fed by a gear pump to a spinneret consisting of an outer tube with a diameter of 1 mm and an inner tube with a diameter of 0.7 mm. Water was introduced into the inner orifice at room temperature to make a lumen of the hollow fiber. The hollow fiber was extruded from the spinneret and wound on a take-up winder after entering into a water bath to induce the phase separation and solidify the membranes. The conditions for membrane preparation are shown in Table I. The PVB concentration, the ratio of PVB to TiO_2, and the coagulation bath composition were changed to obtain various asymmetric porous membranes. The hollow fiber membranes were kept in water and exposed to fluorescent light (220 V, 88 W) for about 12 h per day.

Characterization of the hollow fiber membrane

To obtain the dry membrane, the composite hollow fiber membranes were freeze-dried with a freeze dryer (EYELA, FD-1000, Japan). The dry hollow fiber membranes were fractured in liquid nitrogen and treated with Au/Pd sputtering. The cross sections and the surfaces of the hollow fiber membranes were examined using a scanning electron microscope (SEM, JSM-5610LVS; Hitachi, Japan) with an accelerating voltage of 15 kV. The mass percentage between carbon and titanium at the membrane surface and cross section was observed by energy dispersive spectrometer (EDS, JSM-5610LVS; Hitachi).

Water permeability through the hollow fiber membrane was measured by a method similar to that described by Saito and coworkers.[31] Pure water was forced to permeate from the inside to the outside of the hollow fiber membrane. The transmembrane pressure was applied by adjusting the pressure valve close to the release side, and pressure was averaged from the readings of the two pressure gauges (ranged from 0.05 to 0.1 MPa). The water permeability was calculated by the following equation:

$$J = V/[A\{(P_1 + P_2)/2\}t] \quad (1)$$

where J is the permeation rate, V is the volume of permeated water, A is the inner surface area of the membrane, t is the permeation time, P_1 and P_2 are the pressures for the inlet and outlet, respectively. Before we started to get the permeability data, the permeation experiment was carried out for 3 min to

TABLE I
The Conditions for Hollow Fiber Membrane Preparation

Extrusion rate of polymer solution	0.11 m/s
Water flow rate in inner spinneret tube	0.23 m/s
Take-up speed	0.18 m/s
Air gap (distance from spinneret to water bath)	30 mm
Coagulation bath temperature	298 K

TABLE II
Polystyrene Latex Particle Number in Solution

Particle size (nm)	Particle concentration (number/mL)
20	1.2×10^{14}
50	2.9×10^{12}
100	1.0×10^{11}
300	4.3×10^{9}

make sure that the water permeation condition was stable.

To measure the rejection property of the membranes, the particle rejection experiment was performed using the same apparatus as that used in the water permeation experiment. The particles used were monodispersed polystyrene latex particles with various diameters of 500, 300, 100, 50, and 20 nm (Duke Scientific, Fremont, CA). The feed solutions were prepared by dispersing the latex particles in water containing an aqueous nonionic surfactant (0.1 wt % Triton X-100). The particle numbers in the solutions are shown in Table II. Since the polystyrene particles cannot be dissolved by water, they existed as dispersed nanoparticles. The particle concentration in the filtrate and feed solution were measured with an ultraviolet (UV) spectrophotometer (U-200; Hitachi) under the wavelength of 385 nm. The particle rejection coefficient R is defined as

$$R = 1 - C_f/C_0 \quad (2)$$

where C_0 and C_f are particle concentrations in the feed and the filtrate, respectively.

The tensile strength and elongation of the hollow fiber membrane were measured with a tensile tester (AGS-J; Shimadzu, Kyoto, Japan). The membrane was fixed vertically between two pairs of tweezers with the length of 50 mm. Then the membrane was extended at a constant elongation rate of 50 mm/min until it was broken.

A contact angle meter (Drop Master 300; Kyowa Interface Science, Niiza, Japan) was used to measure the contact angle of water on the outer surface of hollow fiber membranes at room temperature. A 0.5 μL of water droplet was dropped on the outer surface of the membranes.

RESULTS AND DISCUSSIONS

Membrane structure

Hollow fiber membrane structures are shown in Figure 2. The structures of both PVB and composite membranes are shown in this figure. Compared with PVB membranes, it is clearly shown that small white particles scattered both on the cross section and on the surface of the composite membrane. These small particles were considered to be TiO_2 particles. It is also shown from SEM that TiO_2 distributed through the composite membrane homogeneously. The PVB membrane has a dense skin, thus no pores can be detected on either surface at this magnification level. There are some pores on the surfaces of the composite membrane because of the addition of TiO_2. Both the PVB membrane and the composite membrane have finger-like cavities in both inner and outer surface sides.

Water permeability

When only 20 h passed after membrane preparation, the water permeability experiment was carried out for the hollow fiber membranes containing different TiO_2 concentration. The results are shown in Figure 3. When the weight ratio of TiO_2 to PVB was less than 1, the water permeabilities of the composite membranes hardly changed. However, when the weight ratio of TiO_2 to PVB was more than 1, especially when PVB concentration is 10 wt %, the water permeabilities of the composite membranes increased with the addition of TiO_2. When PVB concentration was 10 wt %, the membranes were usually weak, especially in the case that the ratio of TiO_2 to PVB was less than 1. Thus only two kinds of membranes for 10 wt % PVB concentration were prepared.

Figure 4 shows the SEM images of the outer surface for the membranes with different TiO_2 concentration. P and T in this figure caption show the polymer and TiO_2, respectively, and the number following to P shows the polymer weight percentage. When the weight ratio of TiO_2 to PVB was lower, there were no pores on the membrane outer surface. On the other hand, when the weight ratio of TiO_2 to PVB was higher, the composite membranes became porous. Generally, it can be said that the pore size of the membrane depends upon the size of such aggregated particles as macromolecules, nodules, or nodule aggregates. The increase in pore size can be roughly estimated from the increase in the roughness and size of aggregated particle observed at the top surface.[32] Young et al. explained the increase in the porosity of the membrane top layer by theories based on the ratio of nonsolvent inflow to solvent outflow.[33] With an increase in the ratio of TiO_2 to PVB, nonsolvent (water) inflow and solvent (DMAc) outflow of the top layer is changed greatly. The existence of a larger amount of TiO_2 also disturbs the aggregation of the polymer molecules in the top layer, yielding a membrane with a more porous top layer. This brought about the higher water permeability in the case of high weight ratio of TiO_2 to PVB, as shown in Figure 3.

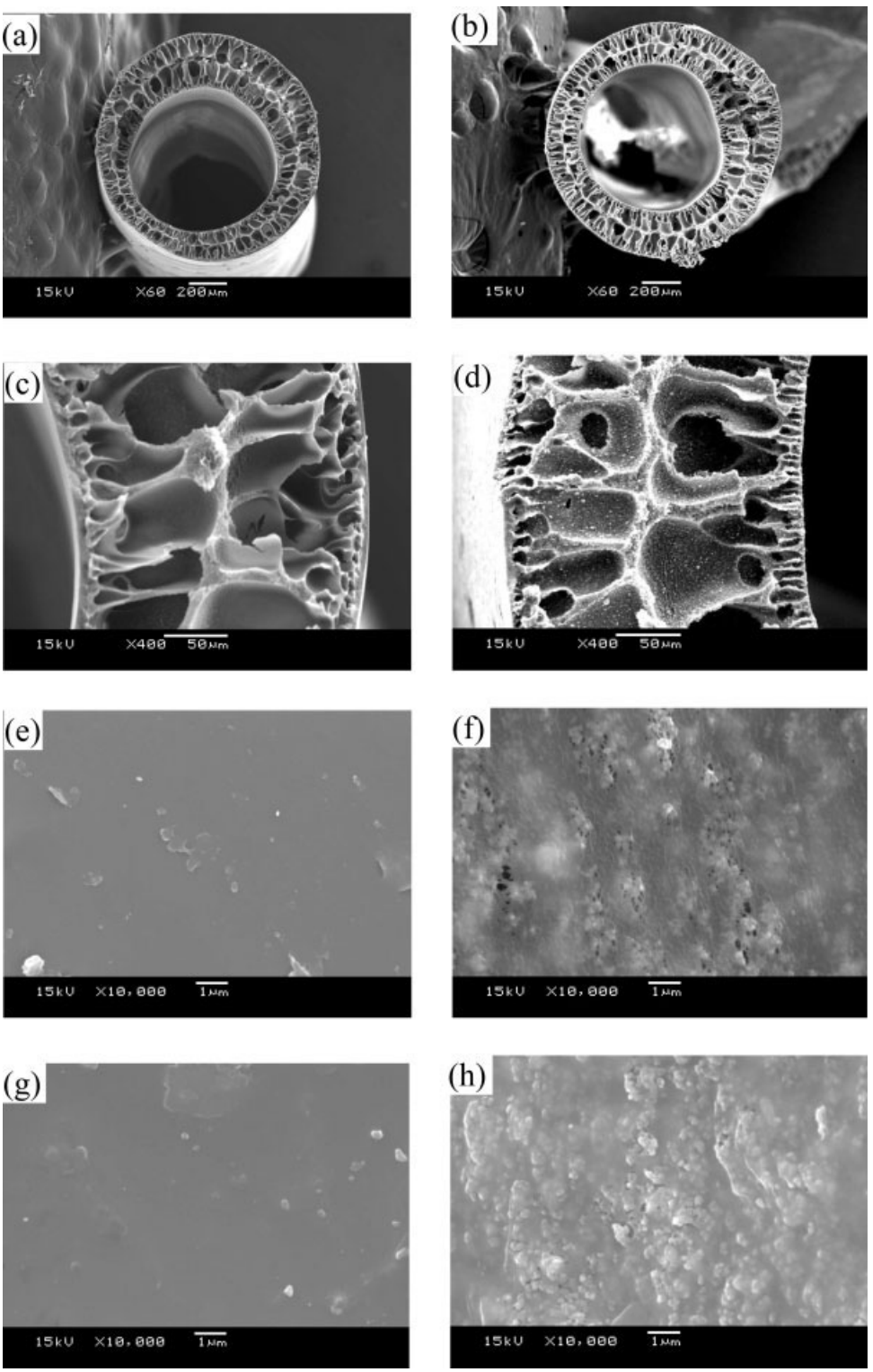

Figure 2 SEM images of the hollow fiber membranes. (a, c, e, g) PVB (15 wt %); (b, d, f, h) PVB (10 wt %) : TiO_2 = 1 : 2. (a, b) Whole cross section; (c, d) enlarged cross section; (e, f) inner surface; (g, h) outer surface.

For all the membranes, the water permeabilities were measured over an extended period. The change of water permeability for the long-term interval is shown in Figure 5. The water permeability of PVB membranes hardly changed over time. On the other hand, we found an interesting result that all the water permeabilities of the composite membranes increased at the initial stage with the passage of

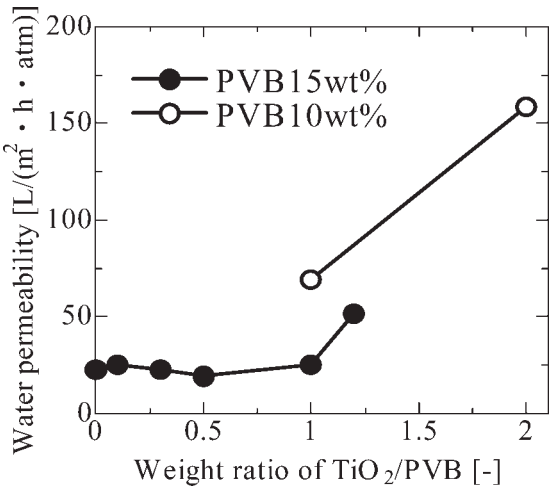

Figure 3 Water permeability for membranes at 20 h after preparation.

time, and became constant when about 15 days passed after membrane preparation.

Figure 6 shows the SEM images of the outer surface for the membrane prepared in the condition of P10 : T = 1 : 2. The membrane structure at the outer surface changed with time. Over time, more TiO_2 appeared on the top layer, the pore size became larger and the top layer became more porous. Since TiO_2 is a photocatalyst, it can decompose polymer when it is exposed to UV radiation. In this experiment, the hollow fiber membranes were exposed to fluorescent light. As a result, TiO_2 worked as photocatalyst and decomposed the polymer. Thus, more TiO_2 appeared on the outer surface and the pore size became larger. To prove this assumption, the membrane properties for the composite membranes placed in a dark atmosphere without light irradiation were also measured. In this case, membrane

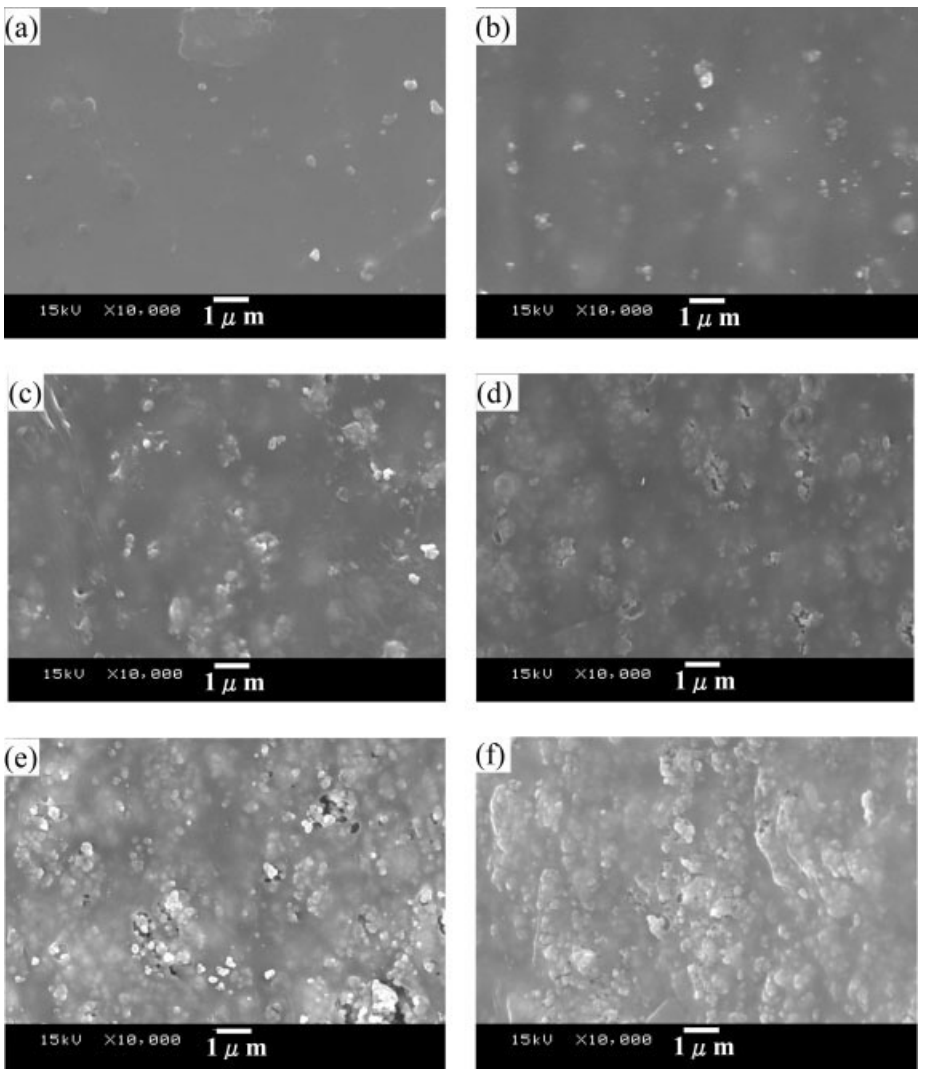

Figure 4 SEM images of the outer surface for the membranes with different TiO_2 concentration, 20 h after preparation. (a) PVB (15 wt %); (b) PVB (15 wt %) : TiO_2 = 1 : 0.1 (P15 : T = 1 : 0.1); (c) P15 : T = 1 : 0.3; (d) P15 : T = 1 : 1; (e) P15 : T = 1 : 1.2; (f) P10 : T = 1 : 2.

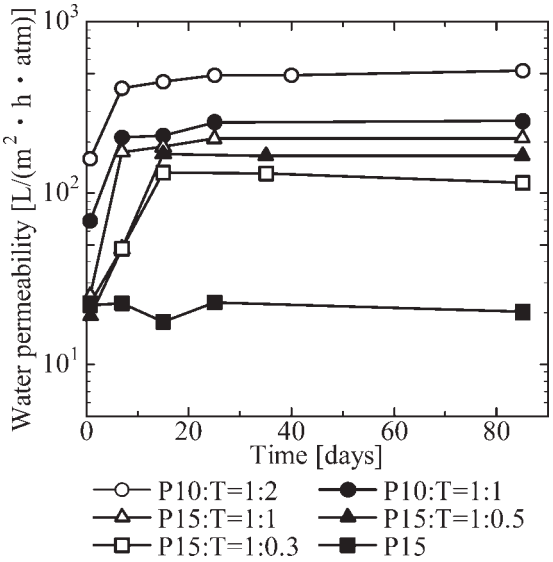

Figure 5 Water permeability for a long term.

properties did not change as time passed. Thus, we reached the conclusion that the polymer on the outer surface was decomposed by light irradiation since TiO_2 is a photocatalyst.

However, all of the top layer structures became similar after 15 days. Thus, the water permeability of the composite membranes increased at first and became constant after 15 days. Not only for membrane (P10 : T = 1 : 2), but for all of the composite membranes, such a phenomenon was found. Furthermore, when polyethersulfone-TiO_2 composite hollow fiber membrane was prepared previously, TiO_2 was also observed to come out onto the membrane top layer after a long period of time. Thus, the photocatalysis of TiO_2 not only worked on PVB polymer, but also on other polymers.

Figure 7 shows the comparison of the water permeability for the membranes at the initial time after preparation and after a long period. As described

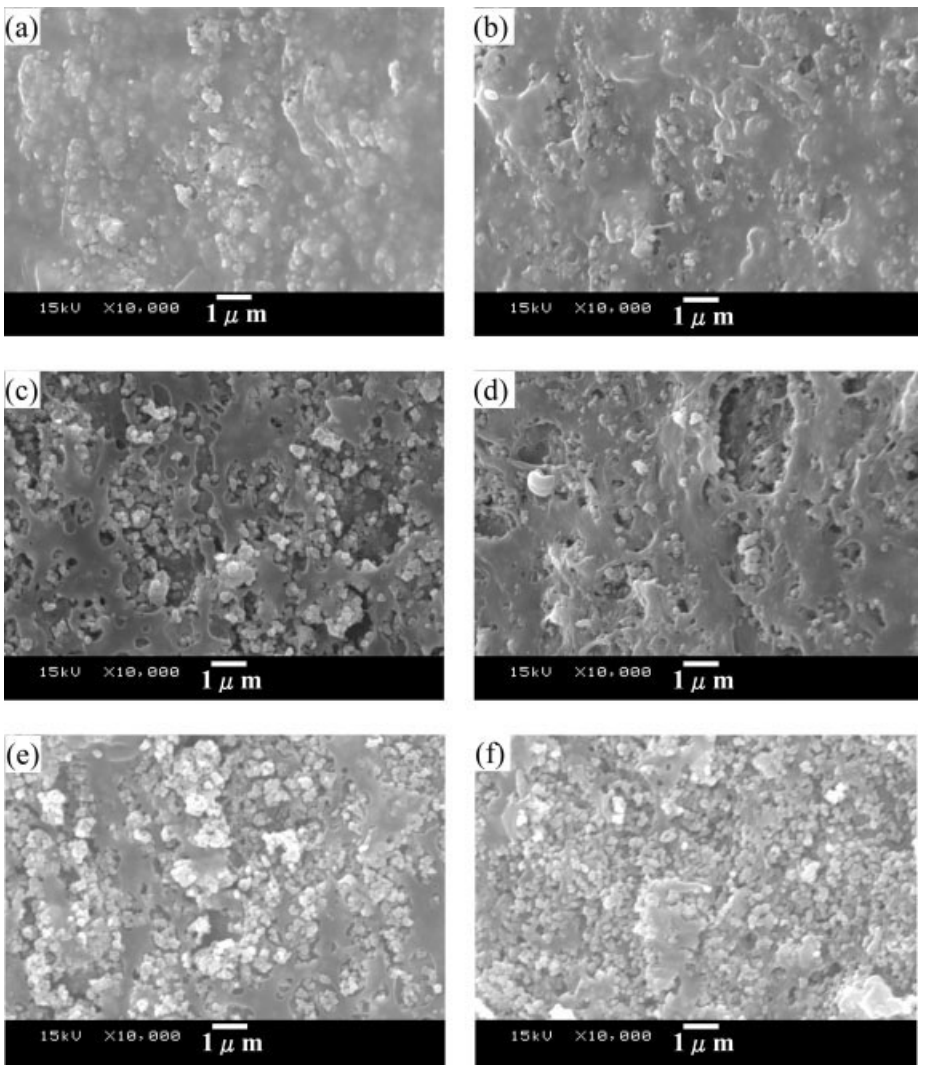

Figure 6 SEM images of the outer surface of membrane P10 : T = 1 : 2. (a) 20 h after preparation; (b) 7 days; (c) 15 days; (d) 25 days; (e) 40 days; (f) 85 days.

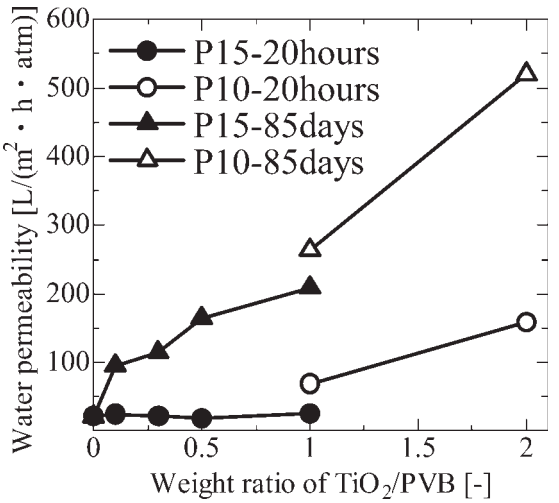

Figure 7 Comparison of the water permeability for the membrane at the initial time and after a long term.

earlier, the water permeabilities hardly changed with the addition of TiO_2 at the initial time after membrane preparation. However, after 85 days the water permeabilities of the composite membranes increased significantly. Moreover, the water permeabilities also increased with the increase of TiO_2. For the membrane (P10 : T = 1 : 2), the water permeability increased more than three times. The largest enhancement factor of about 8 was obtained for the membrane (P15 : T = 1 : 1).

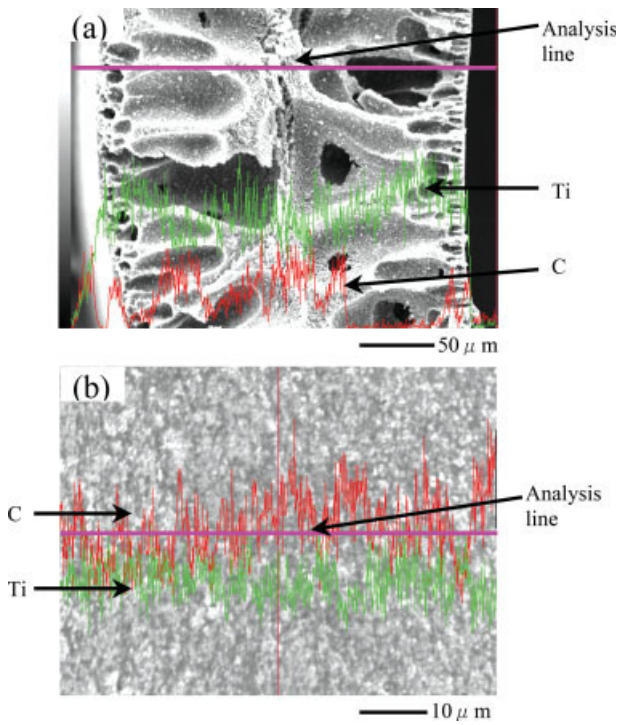

Figure 8 EDS result of line analysis for membrane P10 : T = 1 : 2, 20 h after preparation. (a) Cross section; (b) outer surface. [Color figure can be viewed in the online issue, which is available at www.interscience.wiley.com.]

TABLE III
Composition on the Outer Surface of the Membrane P10 : T = 1 : 2

Time	C : T (wt %)
20 h	60.7 : 39.3
7 days	34.4 : 65.6
15 days	32.2 : 67.8
85 days	29.9 : 70.1
Theoretical value	35.2 : 64.8

EDS results

Figure 8 shows the EDS result of line analysis in the cross section and outer surface of the composite membrane. It is clearly shown that titanium element distributed homogeneously on both the cross section and outer surface.

The EDS analysis of the outer surface of the composite membrane (P10 : T = 1 : 2) showed that the composition of the outer surface changed over time, which is illustrated in Table III. The weight ratio of carbon to titanium on the membrane outer surface was higher than the theoretical value after 20 h. Thus, more polymers covered the membrane outer surface just after the membrane preparation. However, the ratio decreased with the passage of time, which means more TiO_2 came out onto the top layer. After 15 days, the weight ratio of carbon to titanium became constant and was slightly lower than the theoretical value. These EDS results were consistent with the outer surface structure change observed by SEM as shown in Figure 6.

Particle rejection

Effects of the addition of TiO_2 on the particle rejection are shown in Figure 9. For each membrane, the

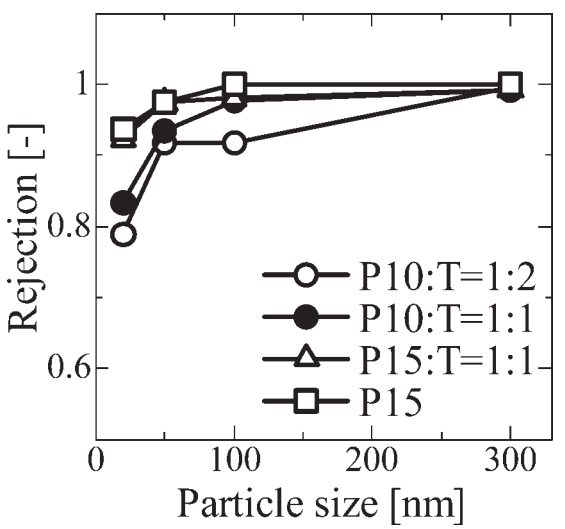

Figure 9 Particle rejection results. Composite membranes at 70 days after preparation.

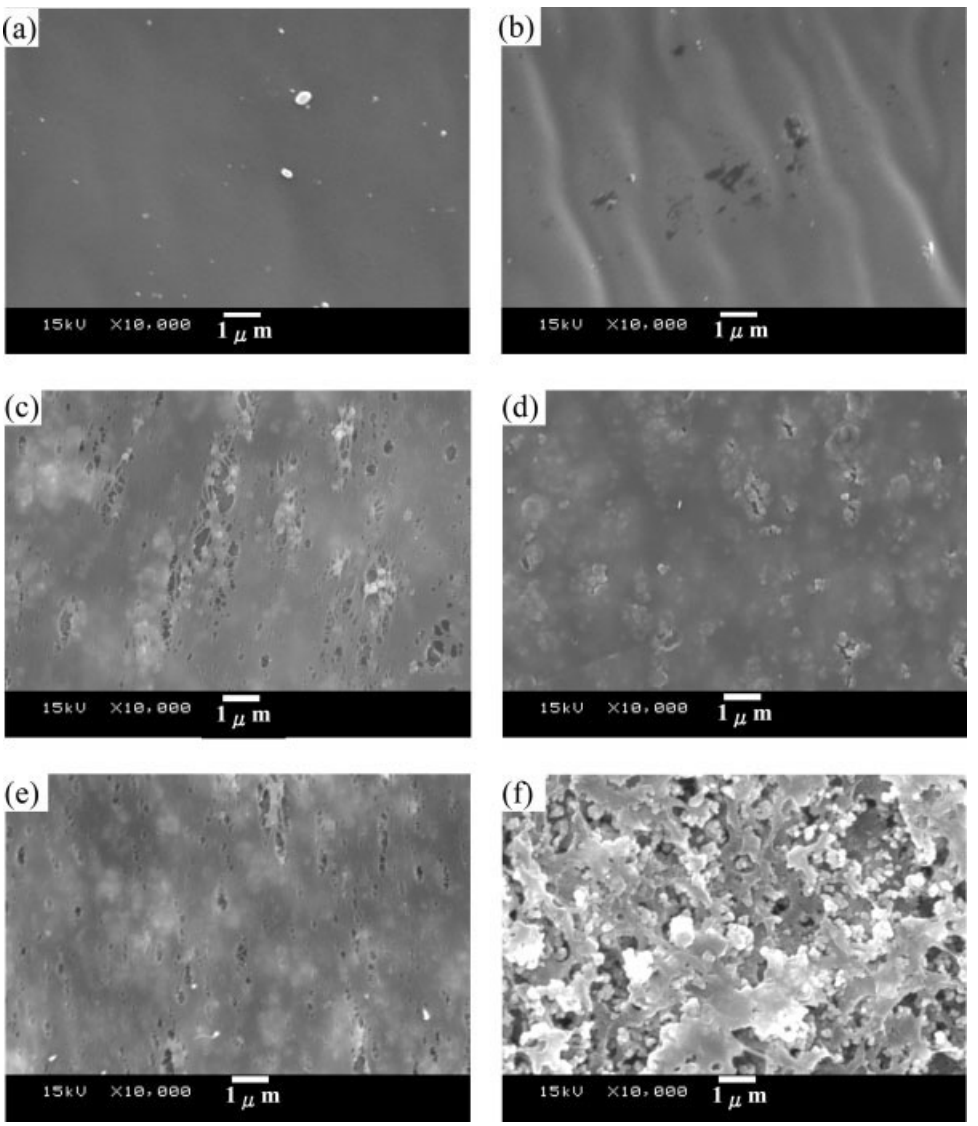

Figure 10 SEM images of the membrane inner surface (a, c, e) and outer surface (b, d, f). (a, b) Membrane (P15), 20 h after preparation; (c, d) membrane (P15 : T = 1 : 1), 20 h after preparation; (e, f) membrane (P15 : T = 1 : 1), 70 days after preparation.

particle rejection experiment was performed for about 30 min by using polystyrene latex particles with different sizes. In this period, the particle rejection hardly changed, suggesting that membrane fouling had not yet occurred. The PVB membranes (□) had high rejection for all sizes of the polystyrene particles. As for the membranes (P15 : T = 1 : 1, △) after 70 days still kept the high particle rejection property, and the rejection data were comparable with those of PVB membrane. For the composite membranes when PVB concentration was 10 wt % (●, ○), the particle rejection decreased a little but remained high for particles larger than 100 nm. Furthermore, even for the 20-nm particles, all of the membranes rejected no less than 80%.

These phenomena can also be explained by the SEM images in Figure 10. Figure 10(a,b) shows the inner and outer surfaces of P15 membrane, respectively; (c) and (d) show the inner and outer surface of the membrane (P15 : T = 1 : 1) after 20 h of membrane preparation; (e) and (f) show the inner and outer surface of the same membrane after 70 days of preparation. There were no pores on either the inner or outer surfaces for P15 membrane; thus P15 membrane had a very high particle rejection. For the membrane (P15 : T = 1 : 1), there were few pores on both the inner and outer surfaces at the initial stage after preparation. However, after 70 days there were many pores on the outer surface formed because of the decomposition of TiO_2, and some of them were larger than 1 μm. On the other hand, the inner surface structure was almost unchanged. UV light could not reach to the inner surface and thus the inner surface structure hardly decomposed. As a result, the

TABLE IV
Contact Angle of Water on Various Membrane Surfaces

Membrane	Contact angle (°)
P15	73.8
P15 : T = 1 : 1 (40 days)	62.8
P10 : T = 1 : 2 (40 days)	56.2
P10 : T = 1 : 2 (85 days)	45.6

composite membrane still kept high particle rejection.

Membrane hydrophilicity

The contact angles of water on the outer surface of the hollow fiber membranes prepared with various concentrations of TiO_2 are shown in Table IV. It is shown that with the increase of the TiO_2 concentration, the contact angle became smaller because TiO_2 is more hydrophilic than PVB. As described earlier, the concentration of TiO_2 appearing on the membrane outer surface increased over time because of the exposure to fluorescent light. Thus the composite membrane became more hydrophilic with the passage of time, as demonstrated when the contact angle of the membrane after 85 days was compared with that after 40 days.

Membrane strength

The tensile strength and elasticity of the hollow fiber membranes are shown in Figure 11. At the initial stage after membrane preparation, both the tensile strength and the elasticity increased with the addition of TiO_2. After 85 days, the tensile strength decreased only a little. With the passage of time, there were more pores on the membrane surface and pore size also became larger. These led to the slight decrease of tensile strength. However, for the composite membranes in the case of TiO_2 : PVB = 1 : 1, tensile strength tested higher than the PVB membranes. The elasticity hardly changed over time. This means that the decomposition of the outer surface was not so serious with respect to the membrane strength.

Comparison with other membrane preparation method for obtaining porous structure at outer surface

As described in the Introduction section, asymmetric membranes can be obtained when water vapor is induced during air gap distance.[22] However, to our knowledge, it is difficult to control the humidity during the air gap distance. Thus, in this study, to have a comparison with the structure of PVB-TiO_2 membrane, solvent was added into a coagulation bath to obtain porous structure at the outer surface. Figure 12 shows the outer surface and cross-section structure of the membranes prepared by various coagulation bath compositions. SEM images of membrane showed that the outer surface of the membrane prepared with higher solvent content in the coagulation bath led to more porous morphology and larger pore size, which consisted with the result obtained by Chou and Yang.[21] However, it was clearly shown by the cross-section structure that when the solvent in the coagulation bath was too much (DMAc : water = 80 : 20, 50 : 50), a suitable membrane structure with round cross-section could not be obtained because of the softness of the membrane. That is, a good hollow fiber membrane could not be prepared in such a condition using the apparatus in our laboratory. In the case of DMAc : water = 25 : 75, the normal membrane structure was obtained. That is, when the ratio of solvent to water in the coagulation bath was less than 25 : 75, the proper membrane could be obtained.

When the solvent was added into the coagulation bath (DMAc : water = 25 : 75), the water permeabil-

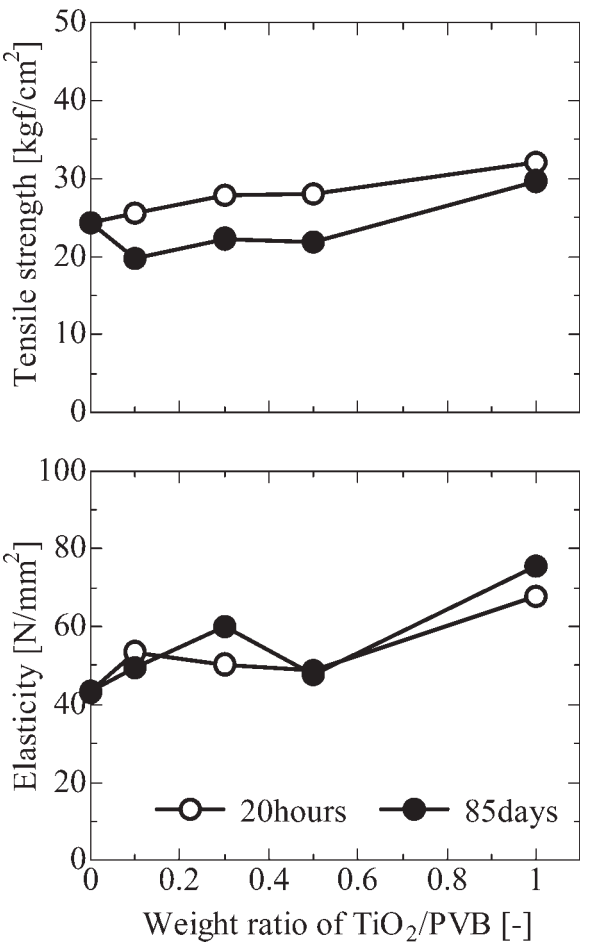

Figure 11 Mechanical strength. Polymer concentration: 15 wt %.

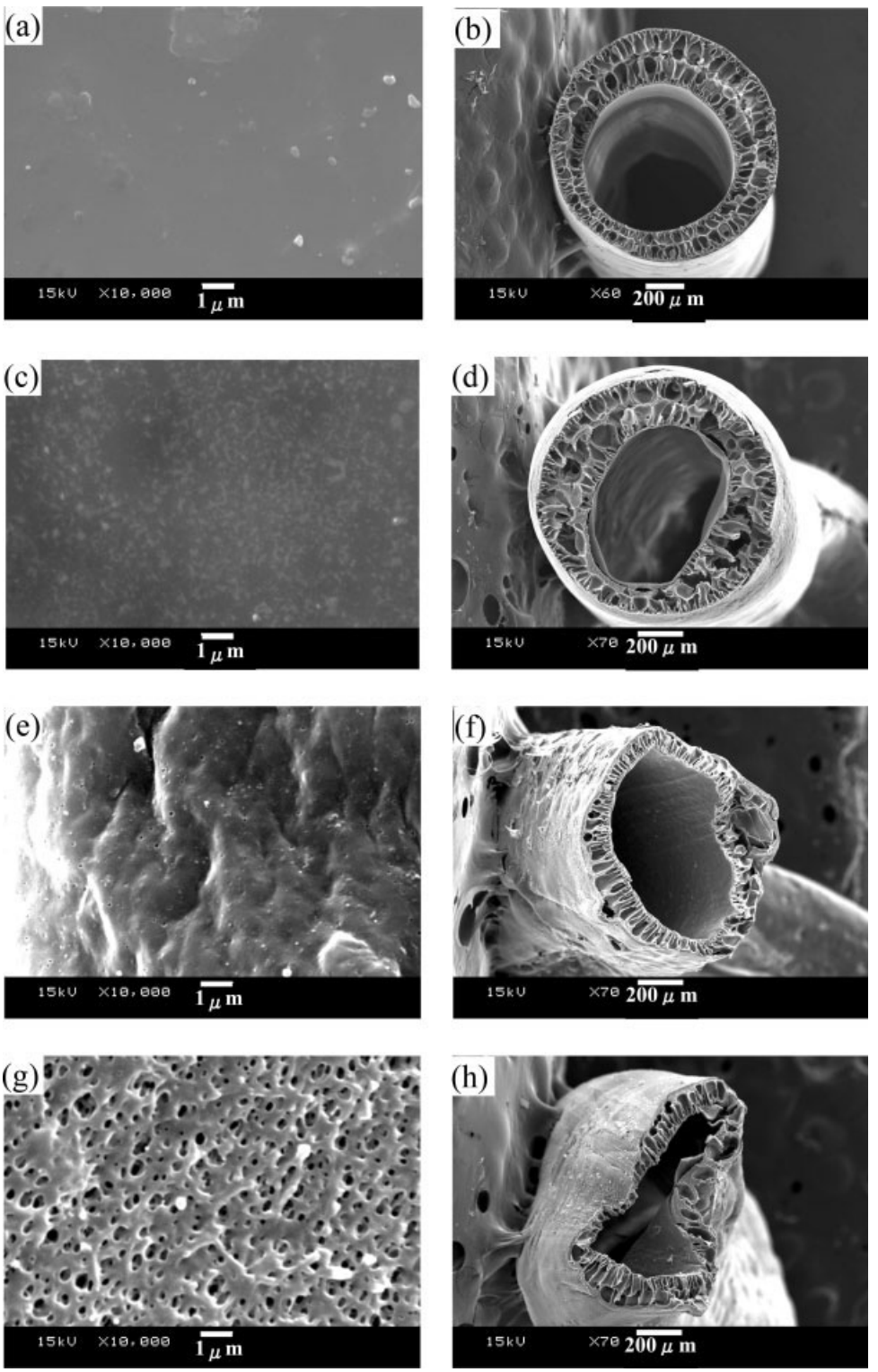

Figure 12 Outer surface (a, c, e, g) and cross section (b, d, f, h) of the hollow fiber membranes. Polymer concentration: 15 wt %; bath composition, DMAc : water (a, b) 0 : 100; (c, d) 25 : 75; (e, f) 50 : 50; (g, h) 80 : 20.

ity for such a membrane (48.8 L m^{-2} h^{-1} atm^{-1}) was higher than that of a PVB membrane (22.4 L m^{-2} h^{-1} atm^{-1}). However, compared with the composite membranes, the increase of water permeability was not remarkable. As described earlier, the addition of TiO_2 brought about eight times higher water permeability. Thus, the addition of TiO_2 is a more useful and simpler way to obtain porous structure at the outer surface than the addition of solvent to the coagulation bath.

CONCLUSIONS

Asymmetric PVB-TiO_2 composite hollow fiber membranes were successfully prepared via the NIPS method.

In all the membranes, finger-like cavities were formed. TiO_2 were dispersed homogeneously in the composite hollow fiber membranes. A small amount of TiO_2 appeared on the membrane surface just after the membrane preparation. However, TiO_2 appeared on the surface under the fluorescent light irradiation and became constant after about 15 days.

Water permeability increased with the addition of TiO_2. The more TiO_2 was added into the dope solution, the higher the water permeability. Under fluorescent light irradiation, water permeability also increased because of the formation of porous structure at the outer surface and became constant after about 15 days. Nonetheless, the composite membrane kept good particle separation property because of the constant dense inner surface.

The water contact angle on the outer surface of the composite membrane was smaller than that of PVB membrane. In addition, the addition of TiO_2 was effective to improve the mechanical property of the hollow fiber membrane.

PVB membranes were also prepared by changing the coagulation bath composition. Under the preparation conditions of our laboratory, appropriate asymmetric PVB hollow fiber membranes were not obtained when the ratio of DMAc to water was more than 50 : 50. In contrast to this, addition of TiO_2 is a more useful and easier method for the preparation of porous structure on the outer surface of the hollow fiber membrane.

References

1. Young, T. H.; Chen, L. W. Desalination 1995, 103, 233.
2. Wienk, I. M.; Boomgaard, Th. V. D.; Smolders, C. A. J Appl Polym Sci 1994, 53, 1011.
3. Kim, J. H.; Lee, K. H. J Membr Sci 1998, 138, 153.
4. Xu, Z. L.; Qusay, F. A. J Membr Sci 2004, 233, 101.
5. Young, T. H.; Huang, Y. H.; Huang, Y. S. J Membr Sci 2000, 171, 197.
6. Han, M. J.; Bhattacharyya, D. J Membr Sci 1995, 98, 191.
7. van de Witte, P.; Esselbrugge, H.; Dijkstra, P. J.; van den Berg, J. W. A.; Feijen, J. J Membr Sci 1996, 113, 223.
8. Shen, F.; Lu, X.; Bian, X.; Shi, L. J Membr Sci 2005, 265, 74.
9. Seymour, S. B.; Carraher, C. E. Polymer Chemistry—An introduction; Marcel Dekker: New York, 1988.
10. Taniguchi, M.; Belfort, G. J Membr Sci 2004, 231, 147.
11. Knoell, T.; Safarik, J.; Cormack, T.; Riley, R.; Lin, S. W.; Ridgway, H. J Membr Sci 1999, 157, 117.
12. Nabe, A.; Staude, E.; Belfort, G. J Membr Sci 1997, 133, 57.
13. Pasmore, M.; Todd, P.; Smith, S.; Baker, D.; Silverstein, J.; Coons, D.; Bowman, C. N. J Membr Sci 2001, 194, 15.
14. Lee, N.; Amy, G.; Croue, J. P.; Buisson, H. J Membr Sci 2005, 261, 7.
15. Denizli, A.; Tanyolac, D.; Salih, B.; Aydinlar, E.; Ozdural, A.; Piskin, E. J Membr Sci 1997, 137, 1.
16. Ma, X.; Sun, Q.; Su, Y.; Wang, Y.; Jiang, Z. Sep Purif Technol 2007, 54, 220.
17. Fu, X. Y.; Matsuyama, H.; Teramoto, M.; Nagai, H. Sep Purif Technol 2005, 45, 200.
18. Fu, X.; Matsuyama, H.; Teramoto, M.; Nagai, H. Sep Purif Technol 2006, 52, 363.
19. Zeman, L. J.; Zydney, A. L. Microfiltration and Ultrafiltration; Marcel Dekker: New York, 1996.
20. Mulder, M. Basic Principles of Membrane Technology; Kluwer Academic: The Netherlands, 1996.
21. Chou, W. L.; Yang, M. C. Polym Adv Technol 2005, 16, 524.
22. Tsai, H. A.; Kuo, C. Y.; Lin, J. H.; Wang, D. M.; Deratani, A.; Pochat-Bohatier, C.; Lee, K. R.; Lai, J. Y. J Membr Sci 2006, 278, 390.
23. Ismail, A. F.; Hassan, A. R. Sep Purif Technol 2007, 55, 98.
24. Xiao, Y.; Wang, K. Y.; Chung, T. S.; Tan, J. Chem Eng Sci 2006, 61, 6228.
25. Yang, Y.; Zhang, H.; Wang, P.; Zheng, Q.; Li, J. J Membr Sci 2007, 288, 231.
26. Luo, M. L.; Zhao, J. Q.; Tang, W.; Pu, C. S. Appl Surf Sci 2005, 249, 76.
27. Watanabe, T.; Nakajima, A.; Wang, R.; Minabe, M.; Koizumi, S.; Fujishima, A.; Hashimoto, K. Thin Solid Films 1999, 351, 260.
28. Yu, J.; Zhao, X. Mater Res Bull 2001, 36, 97.
29. Jeon, J. D.; Kim, M. J.; Kwak, S. Y. J Power Sources 2006, 162, 1304.
30. Genne, I.; Kuypers, S.; Leysen, R. J Membr Sci 1996, 113, 343.
31. Iwata, H.; Saito, K.; Furusaki, S.; Sugo, T.; Okamoto, J. Biotechnol Prog 1991, 7, 412.
32. Kim, J. H.; Lee, K. H. J Membr Sci 1998, 138, 153.
33. Young, T. H.; Chen, L. W. J Membr Sci 1991, 59, 169.